

EFFICIENT MULTISCALE PREDICTION OF CANTILEVER DISTORTION BY SELECTIVE LASER MELTING

C. Li, J. F. Liu, Y.B. Guo*

Dept. of Mechanical Engineering, The University of Alabama, Tuscaloosa, AL35487, USA

Abstract

Large tensile residual stress is one major issue for metal components made by selective laser melting (SLM). Residual stress is induced by non-uniform heat input, which leads to part distortion and detrimentally affects product performance. The conventional single track simulation method is not feasible to predict the distortion of a macro part since it demands an exceedingly long computational time. The coupling multiphysics phenomenon during the SLM process further complicates this issue. In this study, a temperature-thread multiscale modeling approach has been developed to predict part distortion of a twin cantilever. An equivalent body heat flux calculated from the micro scan model was imported as the “temperature-thread” to the subsequent layer hatch model. Then the hatched layer with temperature field can be used as a basic unit to build up the macro part. The temperature history and residual stress fields during the SLM process were predicted. And the distortion of twin cantilever was calculated with a reasonable accuracy compared to the experimental data.

Keywords: Selective laser melting, distortion, multiscale simulation, additive manufacturing

1. Introduction

Selective laser melting (SLM) is capable of producing near full density metallic functional component directly from CAD data [1,2]. In a typical commercial SLM machine, the powder material is locally melted by a fast moving laser source (scan speed up to 15 m/s). The non-uniform heat input as well as the rapid heating and cooling in the material would generate large amount of tensile residual stresses in the component, which leads to part distortion and cracks [3,4]. Part distortion due to tensile residual stress is one of the major problems of SLM parts. It not only reduces the part geometrical accuracy but also and detrimentally affects the functional performance of the end-use parts.

Several experimental works have been done to systematically investigate the formation of part distortion during SLM process. Kruth *et al* [5] studied the thermal deformation of a 1 mm thickness substrate with one layer of iron powder deposited. Six different scanning strategies were taken into account, and island scanning strategy was proved to cause less distortion than that of the line scanning strategy. Kruth *et al* [6] identified the residual stress and part distortion of SLMed part using bridge curvature method. After the part was removed from the substrate, the part distortion in terms of angle α of the two bottom surface was measured to represent the

* Corresponding author

Tel.: 1-205-348-2615; fax: +1-205-348-6419. E-mail address: yguo@eng.ua.edu

magnitude of thermal residual stress generated inside the component. Several parameters were studied including the length of scan vectors and rotation angle of scan vectors for two sequential layers. It has been found that a shorter scan vectors length and larger rotation angle tend to generate less deformation during the SLM process. Buchbinder *et al* [7] studied the method of reducing distortion of an aluminum twin cantilever by preheating the substrate (see Fig. 2). The cantilever which is an overhang structure can be distorted easily during the SLM process, thus a support structure was designed to minimize the deformation of the cantilever during the process. The cantilever distortion was measured after the support structure was removed from the substrate. Different cantilever bar thickness and preheating temperatures are investigated. A significant reduction of the cantilever distortion was observed when the substrate was preheated to 150 °C.

To have a fundamental understanding of distortion mechanism for SLM processed part, numerical modeling as a powerful tool has been widely used to predict residual stress and part distortion in SLM. Simulation works have been done on a small domain (usually single track or single wall). Dai *et al.* [8] simulated the effect of powder-to-solid transition to investigate the residual stress and distortion of metal and ceramic powders at the micro-scale. Hodge *et al.* [9] studied the thermal and mechanical history of a SLM process on the meso-scale (12 layers of powder). A volumetric moving flux was used to melt powder materials with material state change taken into consideration during the process. Aggarangsi *et al.* [10] explored the residual stress reduction method of a SLMed thin-wall structure by using a secondary moving heat flux to preheat the powder material in a finite element model. Heigel *et al.* [11] studied the thermal history and mechanical response of a single wall deposited on a single-side fixed substrate, the deflection history of the substrate was simulated and validated.

Several studies predicted residual stress and part distortion in SLM on the macro part scale. Zaeh *et al.* [12] applied a uniform thermal load adjusted from experimental data to heat up 20 real layers at the same time to predict the temperature and residual stress field of a cantilever with support on the substrate. Denlinger *et al* [13] applied a hybrid quiet inactive element activation strategy to perform 3D thermal-mechanical analysis of large parts on the order of meters. The distortion of the large part was validated with an electron beam deposited part. Prabhakar *et al.* [14] directly applied a uniform heat source simultaneously to the whole layer to simulate the residual stress formation of tensile test coupons produced by electron beam melting (EBM) as well as the distortion of the substrate. Li *et al* [15-17] developed a stress-thread based multiscale simulation approach to fast predict part distortion, the temperature field of a melt pool was obtained through a single laser scan model and then mapped to a 5 mm by 5 mm small domain from which a local residual stress field was calculated and extended to a macro part model with different scanning strategies considered to predict distortion on a macro level, but only one layer was deposited on the substrate.

Thermal stress prediction for several single tracks on a micro-scale using a fine mesh would take several hours to complete, and it depends on the model size and computer performance. Moreover, a practical SLM part on the macro-scale is generally consist of millions of micro-scale laser tracks which dramatically increases the computational time for the coupled analysis.

Therefore, it is extremely difficult to predict part distortion of a practical SLM part if every single tracks is modeled even a powerful work station is applied.

The objective of this study is to develop a temperature-thread multi-scale finite element approach for efficient predicting part distortion and residual stress for a practical SLM processed part by: (a) developing a novel equivalent heat source for a micro-scale single laser scan model; (b) modeling the power-liquid-solid material state transition phenomena during the SLM process; (c) predicting the residual stress field and distortion of a practical part on a macro-scale model; and (d) validating the predicted distortion with the experimental data.

2. Multiscale Simulation Methodology

2.1 Simulation framework

A multi-scale modeling approach (Fig. 1) is highly needed to predict practical part distortion and residual stress with low computational cost and acceptable accuracy. The temperature-thread multi-scale approach developed in this study can be described in three scales, i.e., micro-scale, meso-scale and macro-scale. In the micro-scale model, a single track is deposited using a laser scan and the temperature history of the melt pool is recorded. In the meso-scale model, the temperature history obtained from the micro-scale model is extended to a single layer. In the macro-scale model, a practical part is built layer upon layer by applying the thermal load developed from the meso-scale model.

The three length scales are integrated through the temperature history “temperature-thread” of the melt material. The temperature information is transferred from the micro-scale model to the macro-scale model using this multiscale method.

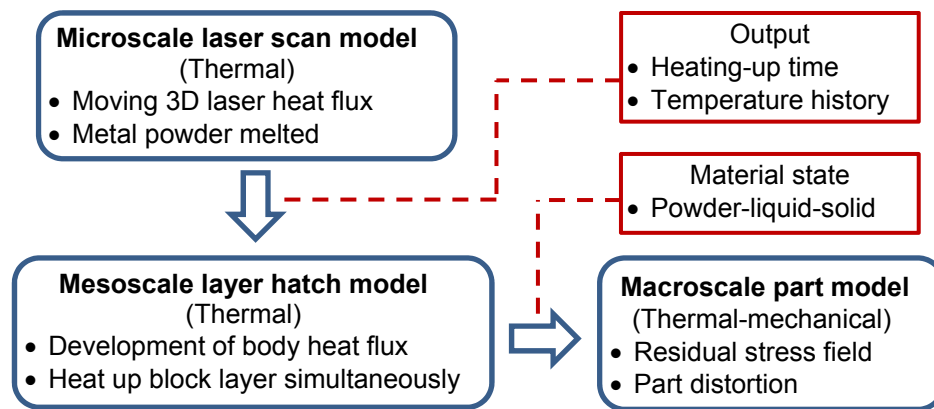


Fig. 1 Multiscale modeling methodology.

The temperature-thread method is described as follows: Firstly, the temperature field of a molten pool was calculated using a moving heat flux to melt powder material placed on the substrate in the micro-scale scan model. Thermal history on the center point of the scan vector is recorded. Secondly, an equivalent heat source is developed based on the thermal history in the

micro-scale scan model, and directly applied to the meso-scale hatch model. Finally, the thermal history of one hatch layer is applied to the macro-scale part model, and each hatch layer is activated one by one until the whole part is built. The total computational time can be dramatically reduced using the multiscale approach compared to the conventional prediction methods.

2.2 Material state transition mechanisms

The twin cantilever (see Fig. 2) was fabricated using an EOSINT M 270 SLM machine equipped with an Yb-fiber laser with a wavelength of 1064 nm. After the part was built, the support structure was removed from the substrate, and then the cantilever distortion was measured. A laser absorption ratio of 0.09 is used [18]. The process parameters are listed in Table 1.

Table 1 SLM process parameters

Laser power	Scan speed	Scan spacing	Layer thickness
W	mm/s	μm	μm
195	800	150	30

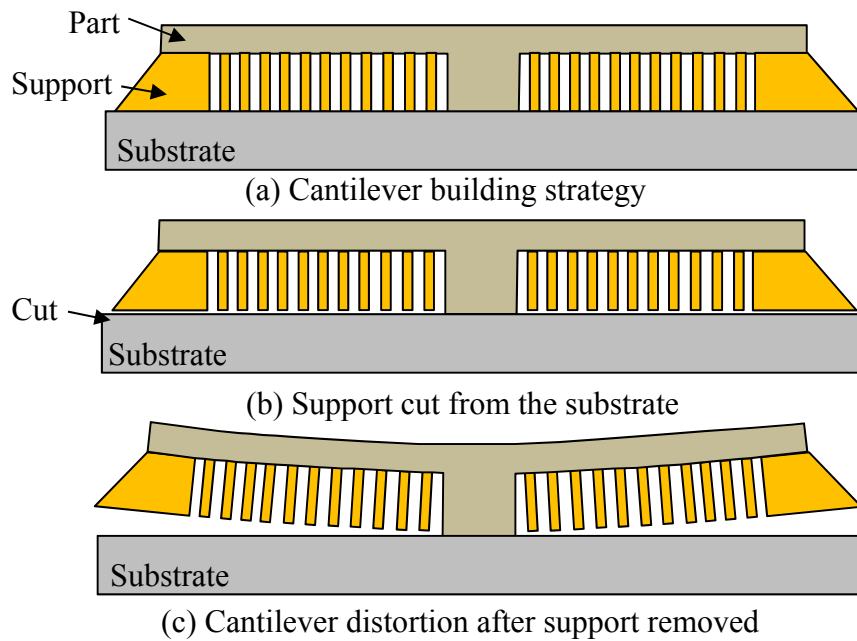


Fig. 2 Distortion of SLM parts: (a) cantilever building strategy, (b) support cut from the substrate, (c) cantilever distortion after support removed.

The metal powder used in this study is a commercial available powder AlSi10Mg. Physical properties of AlSi10Mg are listed in Table 2 [19]. The temperature-dependent thermal material properties were used to ensure calculation accuracy, are listed in Table 3. The plasticity of solid AlSi10Mg was obtained from literature [20], from which the AlSi10Mg tensile test samples were

fabricated by SLM process. The yield point of the material at 600 °C is assumed to 1/10 of that at room temperature. Plasticity properties are listed in Table 4. The substrate used in this study is an AlSi1MgMn plate.

Table 2 Physical properties of AlSi10Mg [19]

Elastic Modulus GPa	Poisson's ratio	Density g/cm ³	Latent heat J/kg	Melting point °C
71	0.33	2.68	389000	600

Table 3 Thermal properties of AlSi10Mg

Temperature (°C)	20	100	200	400
Solid conductivity (W/mK)	110	150	159	155
Specific heat (J/kg °C)	739	922	797	922

Table 4 Plasticity of SLM processed solid AlSi10Mg [20]

Temperature (°C)	Stress (MPa)	Plastic strain
20	200	0
20	300	0.01089
600	20	0
600	30	0.01089

ABAQUS subroutine USDFLD was used to simulate the material state transition (powder-liquid-solid) during the SLM process. The subroutine is coded based on the SLM temperature history and powder's melting temperature. Different properties for powder, liquid, and solid state materials were modeled based on the corresponding material state functions.

2.3 Multiscale simulation models

Micro scan model: In the micro-scale scan model, the temperature field of the melt pool was calculated using the commercial FEA package ABAQUS/Standard. A moving Gaussian distributed heat flux (see Fig. 3a) is developed to model the heat input of the scanning laser in the micro scan model. The power intensity of heat source is determined by laser absorption coefficient A of the powder material, laser power P , laser spot size d_s and the coordinates of the laser spot center (x, y) . The thermal history of the center point of the scan track was recorded as shown in Fig. 3a.

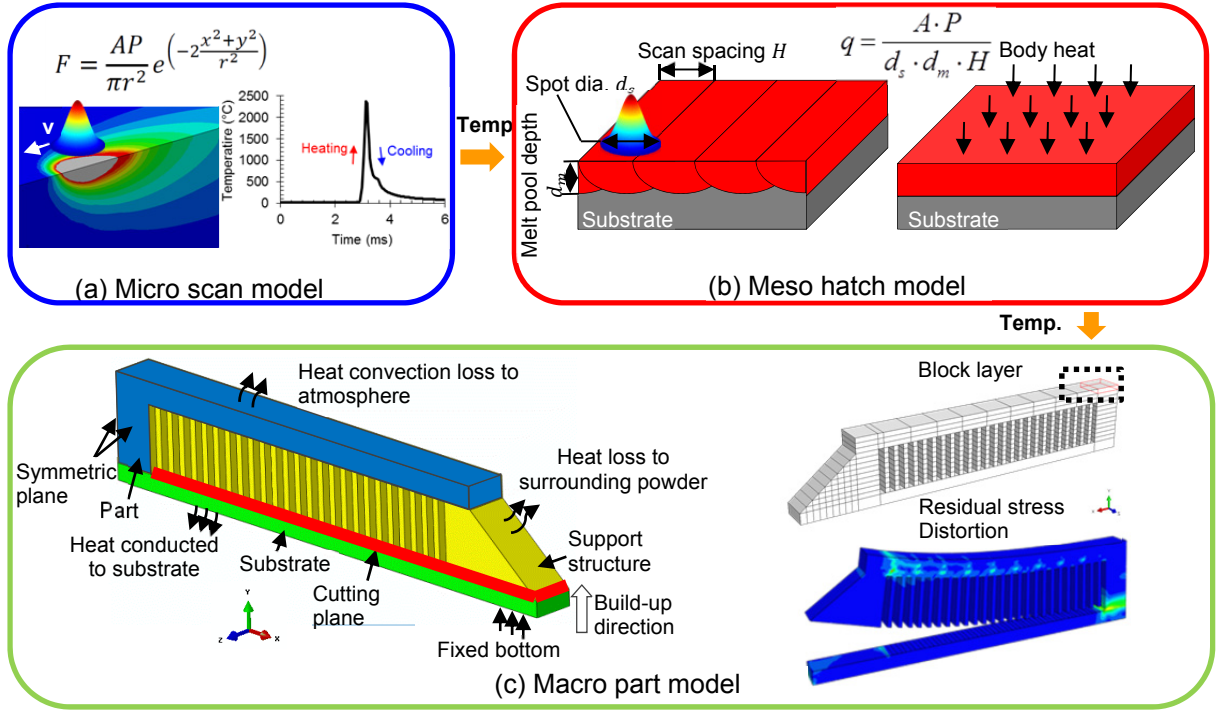


Fig. 3 Over-view of temperature-thread multiscale modeling approach.

Meso Hatch Model: The shape of the melt pool was simplified to a cuboid with a length of laser spot diameter, a width of scan spacing, and a depth of melt pool. The equivalent body flux was defined as the power density (W/m^3) which represents the input power for unit volume of melt material. Based on the thermal history of the melt pool calculated from the micro scan model, an equivalent heat source model was developed as shown in Fig. 3b. The total exposure time of the heat source in the meso hatch model is represented by the total heating time obtained in the micro scan model. The heat input was modeled as a body heat flux q which is associated with laser power P , laser absorption coefficient A , laser spot diameter d_s , melt pool depth d_m , and hatch spacing H . The body heat flux q was given by Eq. (1):

$$q = \frac{A \cdot P}{d_s \cdot d_m \cdot H} \quad (1)$$

Macro Part Model: One quarter of a twin cantilever with support structure was modeled as shown in Fig. 3c. The initial temperature of both the powder and substrate was set to 20°C . The bottom surface of substrate was fixed during the SLM process. Three heat transfer mechanisms were modeled in the macro part model, i.e., heat conduction to the substrate, heat convection of the melt pool to the surrounding powder bed and atmosphere, and heat radiation to the atmosphere.

In this study, the part along with the support was sliced into 12 layers in Y direction (part build-up direction as shown in Fig. 3c). At the very beginning of the simulation, all the elements in the part and support regions were deactivated. When the first powder layer was placed, the

corresponding elements set was activated and heated up by the equivalent body flux for 0.4 milliseconds (exposure time calculated from the micro scan model). A cooling cycle for the whole model with 10 seconds was added right after the heating cycle. Then a new powder was added, heated up, and cooled down to room temperature. This adding-heating-cooling cycle stopped until the whole part was built. At last, the elements located in the cutting plane were deactivated in the model to simulate the process of removing the support structure from the substrate. In order to predict the distortion of the cantilever after the SLM process, the cutting plane was removed by deactivating the associated elements in the plane to release the internal residual stress after the whole part including the support was build. A final distortion of the cantilever will be captured and compared to the experimental measurement.

3. Model Prediction and Discussions

3.1 Material state transition

The material state contours and the corresponding temperature fields during the cantilever building process are shown in Fig. 4. The newly added powder material (in green) was placed on top surface of the cantilever and heated by the equivalent body heat flux. When the temperature went up and was higher than the melting point, the powder started to melt and the state of the material changed to liquid (in red). After the powder was heated for 0.4 milliseconds, the body heat flux was taken off and the material state is all in liquid. Then a cooling period which is ten seconds long was followed. During cooling, the liquid material began to solidify to solid material (in blue). Some of the solid material in the previous layer was remelted when heating up the next layer as shown in Fig. 4d. At last, the liquid was fully solidified and the whole model was cool down to room temperature.

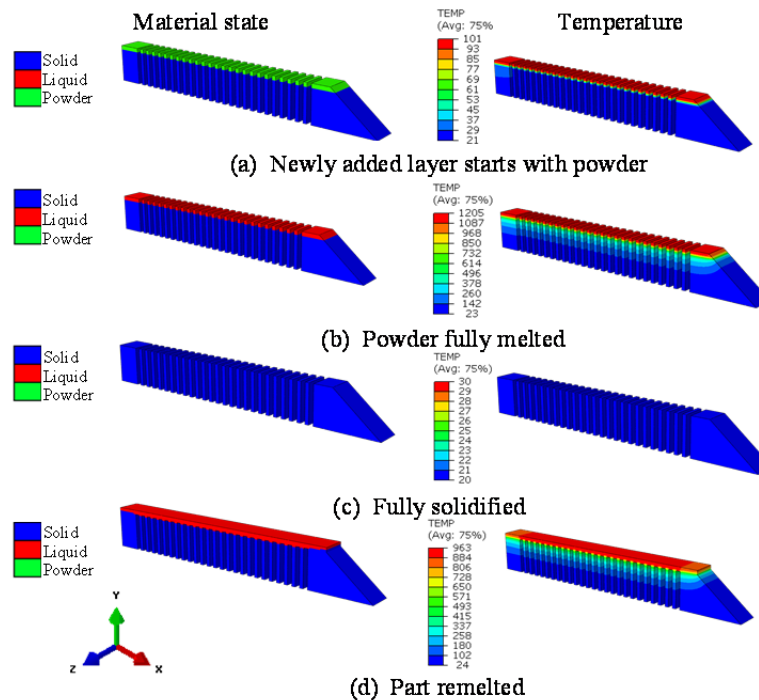


Fig. 4 Material state and temperature field evolution during layer build up.

With support on the substrate, a large tensile residual stress S_{11} was observed on the upper layer of the cantilever as shown in Fig. 5a. Also, the normal stress S_{11} which is perpendicular to the part building direction, dominates the three normal stress components. This could be explained by the temperature gradient mechanism [5]. During the heating cycle, the expansion of the top layer of the cantilever was restricted by its surrounding material and compressive stress was induced. When the top layer cools down, the contraction of the top layer was then constrained, which leads to tensile residual stress on the top layer of the cantilever. After the support was cut from the substrate, normal stress (S_{11}) in X direction on the top layer of the substrate becomes compressive. It was caused by the plastic deformation of the cantilever arm after equilibrium residual stress state was broken inside the as-build cantilever.

3.3 Part distortion

In the experiment, the measurement points for distortion were located on the top surface of the twin cantilever along longitudinal direction. To compare with the measured distortion, a nodal path located on the top surface of the cantilever along the distortion direction (Z) was created in the simulation shown as the black dots in Fig. 6.

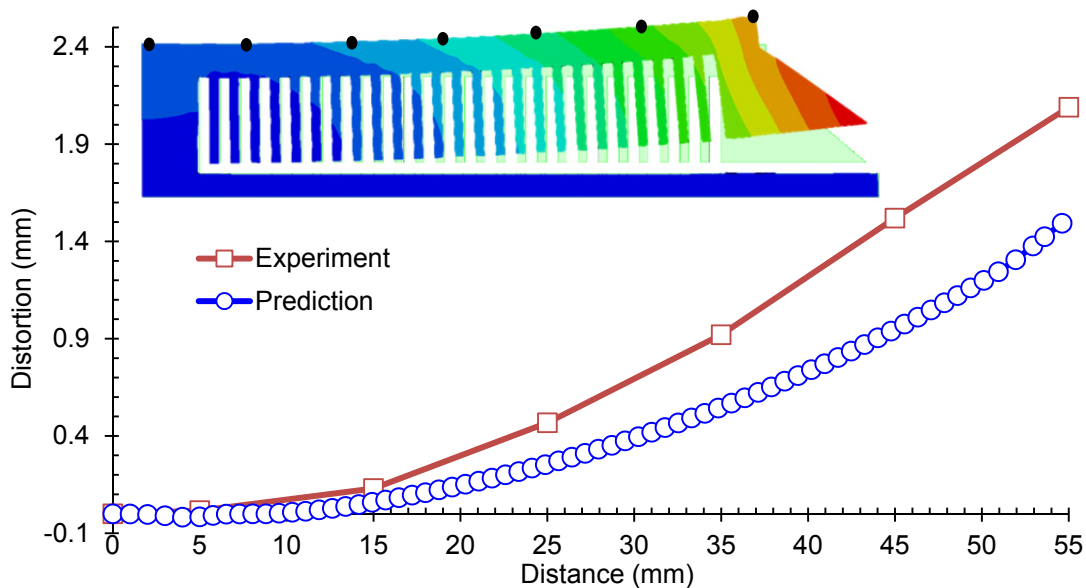


Fig. 6 Part distortion validation: prediction vs measurement.

After the support was removed from the substrate, the cantilever bends towards the build direction, a concave up shape curve was observed. The predicted distortion and the experimental data show same bending direction and similar magnitude of distortion. The formation of this curve is due to the thermal history of the twin cantilever. The material located in the upper layer of the cantilever was expanded due to the laser heating. When the material cools down, the plastic strain in the upper layers became smaller than the lower layers, and a large tensile residual stress was induced in the upper layer areas. After the support was removed, most of the tensile residual stress was released and the cantilever reached a stable state. Then, a concave shaped distortion was formed. The maximum distortion in the experimental was 2.1mm while

the predicted maximum distortion was 1.5 mm, which means an error of about 28 % was obtained. One possible reason could be the input heat source underestimated the actual laser heat input during the SLM experiment. Furthermore, the number of sliced layers has been reduced from approximately 400 in the experiment to 12 in the macro part model. If more sliced layers were used in the simulation, one could expect more accurate predictions.

4. Conclusions

A temperature-thread efficient modeling approach has been developed for fast prediction of a cantilever distortion produced by SLM. Thermal information has been transferred through micro-scale laser scanning, meso-scale layer hatching, and macro-scale part build-up. The predicted distortion of the twin cantilever was compared with the experimental data. The key findings of this study are summarized as follows:

- An equivalent heat source has been developed from the thermal history of melt pool in micro-scale laser scan model and applied to the meso-scale hatch layer, which is incorporated in the macro-scale part to predict part distortion.
- The material state transition phenomenon (powder-liquid-solid) during the SLM process was modeled using different field functions based on the temperature history, maximum temperature and melting temperature of the material.
- Large tensile residual stress was found on the top layer of the part with support on the substrate. After the support was removed, tensile residual stress in the upper layer of the cantilever decreased by 70%.
- Same distortion trend with a maximum distortion error of 28% was predicted when compared to the experimental data.

5. References

- [1] J. Kruth, M. Leu, T. Nakagawa, 1998, Progress in additive manufacturing and rapid prototyping, *CIRP Annals-Manufacturing Technology*. 47(2):525-540.
- [2] G. N. Levy, R. Schindel, J. Kruth, 2003, Rapid manufacturing and rapid tooling with layer manufacturing (LM) technologies, state of the art and future perspectives, *CIRP Annals-Manufacturing Technology*. 52(2):589-609.
- [3] M. Shiomi, K. Osakada, K. Nakamura, T. Yamashita, F. Abe, 2004, Residual stress within metallic model made by selective laser melting process, *CIRP Ann. Manuf. Technol.* 53(1):195-198.
- [4] P. Mercelis, J. Kruth, 2006, Residual stresses in selective laser sintering and selective laser melting, *Rapid Prototyping Journal*. 12(5):254-265.
- [5] J. Kruth, L. Froyen, J. Van Vaerenbergh, P. Mercelis, M. Rombouts, B. Lauwers, 2004, Selective laser melting of iron-based powder, *J. Mater. Process. Technol.* 149(1):616-622.
- [6] J. Kruth, J. Deckers, E. Yasa, R. Wauthlé, 2012, Assessing and comparing influencing factors of residual stresses in selective laser melting using a novel analysis method, *Proc. Inst. Mech. Eng. Pt. B: J. Eng. Manuf.* 226(6):980-991.

- [7] D. Buchbinder, W. Meiners, N. Pirch, K. Wissenbach, J. Schrage, 2014, Investigation on reducing distortion by preheating during manufacture of aluminum components using selective laser melting, *J. Laser Appl.* 26(1):1-10.
- [8] K. Dai, L. Shaw, 2004, Thermal and mechanical finite element modeling of laser forming from metal and ceramic powders, *Acta Materialia.* 52(1):69-80.
- [9] N. Hodge, R. Ferencz, J. Solberg, 2013, Implementation of a thermomechanical model in diablo for the simulation of selective laser melting, .
- [10] Aggarangsi P, Beuth JL, 2006, Localized preheating approaches for reducing residual stress in additive manufacturing. *In Proc. SFF Symp* 709-720.
- [11] J. C. Heigel, P. Michaleris, E. W. Reutzel, 2015, Thermo-mechanical model development and validation of directed energy deposition additive manufacturing of Ti-6Al-4V, *Additive Manufacturing.* 5(0):9-19.
- [12] M. F. Zaeh, G. Branner, 2010, Investigations on residual stresses and deformations in selective laser melting, *Production Engineering.* 4(1):35-45.
- [13] E. R. Denlinger, J. Irwin, P. Michaleris, 2014, Thermomechanical modeling of additive manufacturing large parts, *Journal of Manufacturing Science and Engineering.* 136(6):061007.
- [14] P. Prabhakar, W. J. Sames, R. Dehoff, S. S. Babu, 2015, Computational modeling of residual stress formation during the electron beam melting process for inconel 718, *Additive Manufacturing.* 7:83-91.
- [15] C. Li, J. F. Liu, Y. B. Guo, 2016, Prediction of residual stress and part distortion in selective laser melting, *Procedia CIRP.* 45171-174.
- [16] C. Li, C. H. Fu, Y. B. Guo, F. Z. Fang, 2016, A multiscale modeling approach for fast prediction of part distortion in selective laser melting, *J. Mater. Process. Technol.* 229703-712.
- [17] C. Li, C. H. Fu, Y. B. Guo, F. Z. Fang, 2015, Fast prediction and validation of part distortion in selective laser melting, *Procedia Manufacturing.* 1355-365.
- [18] E. Louvis, P. Fox, C. J. Sutcliffe, 2011, Selective laser melting of aluminium components, *J. Mater. Process. Technol.* 211(2):275-284.
- [19] EOS GmbH, 2011, Material data sheet: EOS aluminium AlSi10Mg for EOSINT M 270, .
- [20] K. Kempen, L. Thijs, J. Van Humbeeck, J.P. Kruth, 2012, Mechanical properties of AlSi10Mg produced by selective laser melting, *Physics Procedia.* 39(0):439-446.